ISSN 1674-1056
http://cpb.iphy.ac.cn
http://iopscience.iop.org/cpb
中国物理 B
Chinese Physics
中国物理 Chinese Physics B

Imaging alignment of rotational state-selected CH_3I molecule

Le-Le Song(宋乐乐), Yan-Hui Wang(王艳辉), Xiao-Chun Wang(王晓春), Hong-Tao Sun(孙洪涛), Lan-Lai He(赫兰海), Si-Zuo Luo(罗嗣佐), Wen-Hui Hu(胡文惠), Dong-Xu Li(李东旭), Wen-Hui Zhu(朱文会), Ya-Nan Sun(孙亚楠), Da-Jun Ding(丁大军), Fu-Chun Liu(刘福春)

Citation: Chin. Phys. B . 2019, 28(2): 023101. **doi:** 10.1088/1674-1056/28/2/023101
Journal homepage: http://cpb.iphy.ac.cn; http://iopscience.iop.org/cpb

What follows is a list of articles you may be interested in

Molecular dynamics simulations of the effects of sodium dodecyl sulfate on lipid bilayer

Bin Xu(徐斌), Wen-Qiang Lin(林文强), Xiao-Gang Wang(汪小刚), Song-wei Zeng(曾松伟), Guo-Quan Zhou(周国泉), Jun-Lang Chen(陈均朗)

Chin. Phys. B . 2017, 26(3): 033103. **doi:** 10.1088/1674-1056/26/3/033103

Theoretical approach to the study of vibrational effects on strong field ionization of molecules with alignment-dependent tunneling ionization rates

Zhang Mei-Xia, Yan Bing, Yang Yu-Jun, Luo Si-Zuo, Zhu Rui-Han, Yang Xue, Ding Da-Jun

Chin. Phys. B . 2015, 24(9): 093302. **doi:** 10.1088/1674-1056/24/9/093302

Nonsequential double ionization of diatomic molecules by elliptically polarized laser pulses

Tong Ai-Hong, Liu Dan, Feng Guo-Qiang

Chin. Phys. B . 2014, 23(10): 103302. **doi:** 10.1088/1674-1056/23/10/103302

Translational, vibrational, rotational enhancements and alignments of reactions H+ClF (v=0–5, j=0, 3, 6, 9) →HCl+F and HF+Cl,at E_{rel}=0.5–20 kcal/mol

Victor Wei-Keh Chao(Wu)

Chin. Phys. B . 2013, 22(10): 103101. **doi:** 10.1088/1674-1056/22/10/103101

The collision energy effect on the stereodynamics of the Ca + HCl→CaCl +H reaction

Wang Li-Zhi, Yang Chuan-Lu, Liang Jing-Juan, Duan Li-Li, Zhang Qing-Gang

Chin. Phys. B . 2013, 22(4): 043101. **doi:** 10.1088/1674-1056/22/4/043101

Imaging alignment of rotational state-selected CH_3I molecule*

Le-Le Song(宋乐乐)[1,2,3], Yan-Hui Wang(王艳辉)[4], Xiao-Chun Wang(王晓春)[1,3], Hong-Tao Sun(孙洪涛)[1,3,5], Lan-Hai He(赫兰海)[1,3], Si-Zuo Luo(罗嗣佐)[1,3], Wen-Hui Hu(胡文惠)[1,3], Dong-Xu Li(李东旭)[1,3], Wen-Hui Zhu(朱文会)[1,3], Ya-Nan Sun(孙亚楠)[1,3], Da-Jun Ding(丁大军)[1,3], and Fu-Chun Liu(刘福春)[1,3,†]

[1] *Institute of Atomic and Molecular Physics, Jilin University, Changchun* 130012, *China*
[2] *Jilin Institute of Chemical Technology, Jilin* 132022, *China*
[3] *Jilin Provincial Key Laboratory of Applied Atomic and Molecular Spectroscopy, Jilin University, Changchun* 130012, *China*
[4] *College of Electronic Science and Engineering, State Key Laboratory on Integrated Optoelectronics, Jilin University, Changchun* 130012, *China*
[5] *General Hospital of FAW, Changchun* 130011, *China*

(Received 27 July 2018; revised manuscript received 7 November 2018; published online 10 January 2019)

We experimentally and numerically investigate CH_3I molecular alignment by using a femtosecond laser and a hexapole. The hexapole provides the single $|111\rangle$ rotational state condition at 4.5-kV hexapole rod voltage. Based on this single rotational state, an enhanced alignment degree of 0.73 is achieved. Our experimental results are in agreement with the simulation results. We experimentally obtain the ion velocity map images and show the influence of the initial rotational-state population. With the I^+ ion images and angular distributions at different pump-probe delay time, the alignment and anti-alignment phenomena are further demonstrated. The molecules will be under field-free conditions when the laser effect disappears completely at the full revival time. Our work shows that the quantum control and spatial control on CH_3I molecules can be realized and molecular coordinate frame can be obtained for further molecular experiment.

Keywords: hexapole, state selection, velocity map imaging, alignment

PACS: 31.15.am, 31.15.ap, 33.15.Mt, 33.15.Kr **DOI:** 10.1088/1674-1056/28/2/023101

1. Introduction

The research of the CH_3I molecular alignment resulting from the single rotational state has attracted considerable attention thanks to its widespread applications, such as above-threshold ionization (ATI),[1] high-order harmonic generation,[2] chemical reaction dynamics,[3] and non-sequential double ionization.[4] Much effort has been devoted to the developing of effective methods that enable us to control the orientation and alignment of molecules. In 1964, Kramer *et al.* attempted to experimentally manipulate the angular distribution of molecules by using hexapole electrostatic fields.[5] Another technique was then developed to align molecules, termed the 'brute-force' method.[6] The disadvantage of 'brute-force' method is that it needs the molecules to possess a large dipole moment.[7] With the development of lasers, a pulsed laser has been shown to provide a relatively high electric field. So the dipole moment induced by the laser field can contribute to the alignment.[8,9] Further rotational state selection technique makes it possible to achieve high alignment from only one rotational quantum state. In general, symmetric top and nearly symmetric top molecules with non-zero dipole moment can be selected in a specific rotational state by passing through a hexapole setup. In practice, polar symmetric top molecules with $|JKM\rangle$ eigenstates can be selected when the product of $KM < 0$. Like the hexapole, a molecular deflector can also be used to achieve relatively high degree of alignment by selecting molecules populated in low-lying rotational states.[10] The combination of a rotational cold supersonic beam and a long hexapole field has achieved an essentially pure rotational state-selection.[11,12]

The non-adiabatic molecular alignment induced by a femtosecond laser has been extensively studied in recent years,[13–15] and it is valuable for some applications such as orbital reconstruction, and steric reaction dynamics, which requires the aligned molecules under field-free conditions. Non-adiabatic alignment occurs when molecules interact with an ultrafast laser. Due to the anisotropy, the molecules tend to align along the laser polarization direction after a certain delay time.[16] In this case, the alignment laser excites most molecules in the beam to the rotational wave packet, and the coherent superposition of the rotational states that will in-phase and dephase in a certain time and alignment revivals (alignment or anti-alignment periodically re-occured after the alignment laser stopped interacting) would be formed. The absence of the aligning laser field can prevent the distortion of molecular alignment caused by the field. Therefore, non-adiabatic alignment in comparison with adiabatic alignment can observe molecular dynamics and align molecules under field-free conditions.[17–19]

Methyl iodide, as a typical molecule with C_{3V} symmetry,

*Project supported by the National Natural Science Foundation of China (Grant Nos. 11574116, 11534004, 10704028, and 11474123) and the Natural Science Foundation of Jilin Province, China (Grant No. 20170101154JC).

†Corresponding author. E-mail: lfc@jlu.edu.cn

© 2019 Chinese Physical Society and IOP Publishing Ltd

has been investigated through a velocity map imaging method by using a nanosecond laser at different wavelengths.[20–23] Graham *et al.*[24] studied the angular distributions of fragment ions generated from the Coulomb explosion of methyl iodide with a 50-fs intense laser pulse (10^{16} W/cm^2). Some Coulomb explosion channels were assigned, and the KERs of CH_3^+ ions from different channels were measured.

In the present work, we explore laser induced non-adiabatic alignment from state selected CH_3I molecules, both theoretically and experimentally. The single rotational state selection is successfully obtained by hexapole and ions detection is performed by the velocity map imaging technique. We obtain the I^+ ions' images at different delay times, and I^+ angular distributions are analyzed. Finally, we realize quantum control and spatial control of CH_3I molecules. With our work, one can obtain molecular coordinate frame for the further study of photo-dissociation, photo-ionization and collision dynamics in molecular experiment.

2. Experiment

The laser system that is used in present work was a Ti:sapphire chirped-pulse amplification system (Coherent) with a 800-nm central wavelength, the pulse duration was 50 fs and an maximum output energy was 4 mJ per pulse at a 1-kHz repetition rate. A pump-probe setup was used to split the laser beam into two: an aligning 'pump' and an ionizing 'probe'. The polarization of both the pump and the probe laser were parallel to the imaging plane and both laser beams were collinearly focused perpendicularly onto the ionization zone by using a 25-cm-focal-length lens. The intensity of each beam was varied continuously by using a half-wave plate and a Glan polarizer which were placed in front of the focusing lens. The temporal evolution of the alignment was obtained by varying the delay time of the probe pulse with respect to the pump pulse which passed through a computer-controlled translation stages.

The molecular beam setup consisted of three chambers (a source chamber, a chamber with the hexapole, and a chamber containing the ion optics and the detector). A supersonic molecular beam was produced by seeding 2.5% CH_3I in Neon at a 1.5-bar (1 bar = 10^5 Pa) stagnation pressure through a 0.5-mm orifice in a pulsed valve (General Valve Series 9) at a 10-Hz repetition rate. The molecular beam passed through a skimmer into the hexapole chamber where the inhomogeneous electrostatic field in the hexapole focused on rotational-state-selected molecules and the molecules crossed at right angles to the laser beam in the reaction region located in the third chamber. A voltage ratio of 100 V/710 V was applied to the repeller and the extractor, and produced a static electric field of about 300 V/cm in the interaction region. Ions or electrons produced in the interaction region were accelerated by a static electric field along the time-of-flight (TOF) mass analyzer axis and projected onto a two-dimensional (2D) detector composed of a microchannel plate (MCP)/phosphor screen (P47) and a charge-coupled device (CCD) camera. The TOF mass spectrum was acquired with a photomultiplier tube (PMT). All of the measured spectra were transferred into a computer for further processing.

3. Theoretical method

The CH_3I is a symmetrical top molecule. Generally, its rotational state is described by $|JKM\rangle$ in which J is the total rotational angular momentum, K is the angular momentum projection on the molecular symmetry axis, and M is the angular momentum projection on the external static electric field. The hexapole state-selection technique relies on the interaction between an inhomogeneous electric field and the molecular electric dipole moment. For a typical experimental electric field inside a hexapole, the symmetric top molecules have predominantly linear first order Stark effects. The forces exerted on the molecules by the electric field govern the molecular motions inside the hexapole. Molecular trajectories follow the Newton differential equation

$$\frac{\mathrm{d}^2 r}{\mathrm{d}t^2} = \frac{-1}{m}\frac{\mathrm{d}W}{\mathrm{d}E}\frac{\partial E}{\partial r}, \tag{1}$$

where $\partial E/\partial r$ is the electric field gradient, and W is the energy including rotational energy W_{rot} and stark energy W_{stark}. The W can be evaluated by solving a secular equation with the quantum perturbation method. One can readily determine the $\mathrm{d}W/\mathrm{d}E$ by using numerical or fitting methods. The radial position is calculated by using the coupled partial derivative E as the molecule traverses the hexapole. The molecular trajectory motions are numerically calculated by using a fourth-order Runge–Kutta routine. Molecules will do periodic oscillation motions in the hexapole. According to this principle, at a certain distance from the end of the hexapole device, we obtain specific molecular beam and achieve the goal of rotation state selection.

After the hexapole, the interaction of the rotational-state-selected molecules with the intense laser fields is calculated by solving the time-dependent Schrödinger equation (TDSE).[25–29] The time-dependent Schrödinger equation describing a molecule in an intense laser field can be given by using the following Hamiltonian:

$$H = H_{\mathrm{mol}} + H_{\mathrm{ind}}, \tag{2}$$

where H_{mol} is the field-free molecular Hamiltonian and H_{ind} is the Hamiltonian describing the laser interaction with the induced dipole moment. In a nonresonant linearly polarized laser field, the interaction from the permanent dipole moment

is zero, the interaction from the induced dipole moment is reduced to the polarized interaction.

$$H_{\rm ind} = -\frac{1}{4}\varepsilon^2(t)\left(\Delta\alpha\cos^2\theta + \alpha_\perp\right), \quad \Delta\alpha = \alpha_\parallel - \alpha_\perp. \tag{3}$$

Here, $\Delta\alpha$ is the difference between parallel $\alpha_\parallel$ and perpendicular $\alpha_\perp$ polarization component respecting to the molecular axis, θ is the angle between the molecular axis and the pump laser field polarization, and $\varepsilon(t)$ is the time profile of the laser field. As the interaction depends only on polar angle θ, the quantum numbers K and M are conserved. The rotational wave function $\Psi(t)$ can be expanded into a sum of free-field rotor eigenfunctions $|JKM\rangle$, *i.e.*,

$$|\Psi(t)\rangle = \sum_J C_J(t)\,|JKM\rangle, \tag{4}$$

$$\mathrm{i}\hbar\frac{\partial}{\partial t}C_J(t) = E_{JK} - \frac{\Delta\alpha\varepsilon^2(t)}{6}\sum_{J'}\langle JKM|D^2_{00}\left|J'KM\right\rangle. \tag{5}$$

In the above equation, E_{JK} is the rotational energy and D^2_{00} is a Wigner rotational matrix.[28,29] The time-dependent Schrödinger equation can be solved by using Runge–Kutta method.[29] Now the laser pulse leaves the system in a coherent superposition of states and the wave packet evolves freely; that is,

$$|\Psi(t)\rangle = \sum_J C_{JKM}(t)\,\mathrm{e}^{-\mathrm{i}E_{JKt}/\hbar}\,|JKM\rangle. \tag{6}$$

The time-dependent orientation and alignment degrees can be calculated with

$$\left\langle\cos^2\theta\right\rangle_{JKM}(t) = \langle\Psi(t)|\cos^2\theta\,|\Psi(t)\rangle \tag{7}$$

and

$$\left\langle\cos^2\theta\right\rangle_{T(t)} = \sum_J\sum_K P(J,K)\sum_M\left\langle\cos^2\theta\right\rangle_{JKM}(t), \tag{8}$$

where $P(J,K)$ is the Boltzmann distribution.[30,31]

4. Results and discussion

In this paper, the laser alignment of the $|1\pm1\pm1\rangle$ state of CH_3I is studied. The notation used here actually gives the absolute value for each quantum number (K and M) as they have the same alignment dynamics, so we use the $|111\rangle$ to represent the $|1-11\rangle$ and $|11-1\rangle$ states and so on. Figure 1 shows the simulation curves of molecular alignment. The temperature is 10 K, and initial rotational states $|111\rangle$, $|211\rangle$, and $|212\rangle$ are chosen, respectively, to compare with the initial alignment of thermal distribution. The CH_3I rotational period is $\tau = 1/(2Bc) = 66.7$ ps for a rotational constant $B = 0.445\ \mathrm{cm}^{-1}$, thus our ion revival delay time is chosen from 0 to 80 ps.

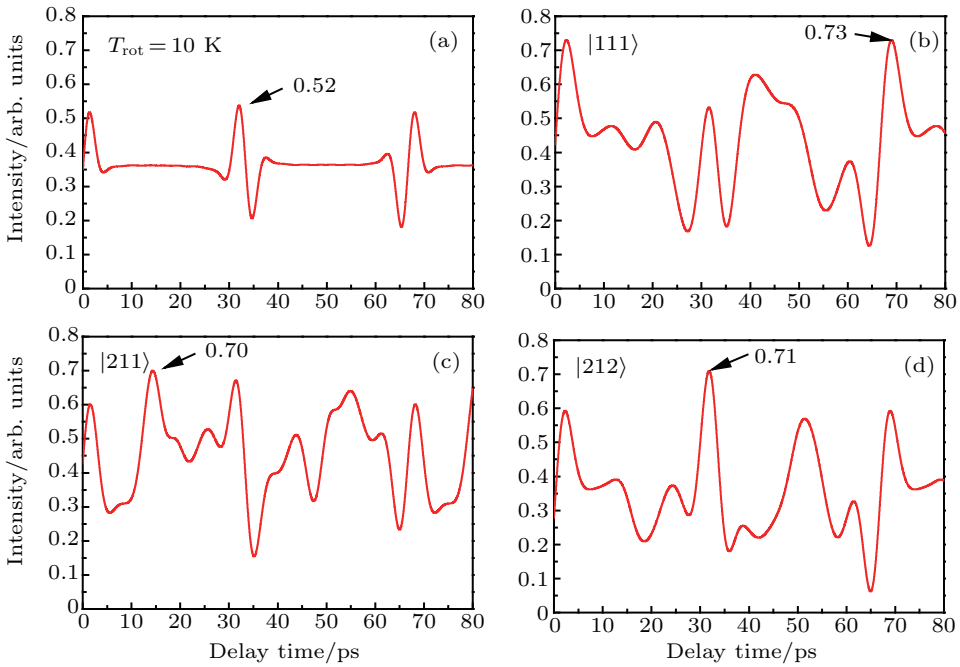


Fig. 1. Time evolutions of initial alignment of CH_3I in different conditions, showing (a) alignment from thermal population with rotation temperature of 10 K, (b)–(d) alignment from different initially populated states at 10 K.

It is found that different revival structures appear when we measure the alignment originating from different initial states. The duration of the single rotation alignment at the 10 K for the molecules is longer than that of thermal distribution. The maximum alignment is present around $\tau/2$ or τ. The simulation shows that the isotropic molecules at 10 K are aligned with a maximum 0.52 alignment degree. This is due to the fact that molecules are populated thermally in a number of incoherent states and the alignment can also be destroyed. Alignment can be increased to a maximum value of 0.73 if

the molecules are initially populated in rotational $|111\rangle$ states at 10 K. Comparing the alignments from Figs. 1(b)–1(d), we can know the degree of alignment $|111\rangle$ is slightly higher than those of alignment $|211\rangle$ and $|212\rangle$ states.

To realize the single rotational state condition, the hexapole is used. Since the Stark energy depends on molecular rotational state and electric field gradient[5,32] in hexapole, the molecular trajectories can be controlled by varying the applied hexapole rod voltage. With the hexapole, spatial focusing can be realized at the position where the molecule interacts with the pump and probe laser beams. The semi-classical trajectories' simulation has been discussed before.[33–35] The simulation and experiment from hexapole focusing are shown in Fig. 2 by giving the yield of the parent ions generated in the laser field (4×10^{12} W/cm^2) as a function of applied hexapole voltage. The rotation temperature of the molecular beam is 10 K according to the simulation focusing curve (black line) and the adjustment of the experimental conditions in Fig. 1. We simulate the rotation states with $J\leq3$, the simulation curve begins to focus at 3 kV, and the first focus peak appears at 4.58 kV, and the first peak of experiment is located at 4.5 kV. Then the experimental signal strength increases only with voltage increasing and no other peak appears. Here we only consider the $J\leq3$, $K=1$ in the simulation, but actually the rotations from $K>1$ also have slight effects in the experiment. The hexapole gives about 5 times amplification for the CH_3I^+ ion enhancement, which indicates that the molecular beam consists of about 80% of CH_3I in the $|JKM\rangle=|111\rangle$ state.

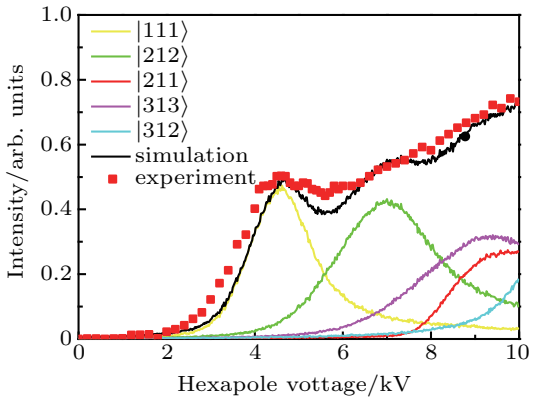


Fig. 2. Simulation and experimental results of CH_3I in the hexapole, with rod voltage scanned from 0 to 10.0 kV.

Figure 3 shows the comparison of revival structure between single rotation state simulation of $|111\rangle$ (Fig. 1(b)) and the normalized experimental data. From Fig. 3, we find that the alignment appears at the delay times 31.85 ps and 68.80 ps when the molecular axis direction is parallel to the laser polarization. The anti-alignment can be obtained at 35.10 ps and 65.35 ps when the molecular axis direction is perpendicular to laser polarization. The simulation trend and structure are in good agreement with experimental results at around 32 ps (half the revival time), and at around 66 ps (full revival time). The alignment degree at full revival time is bigger than half the revival time because the laser effect does not disappear at all at half the revival time. And the molecules is under field-free condition at the full revival time. We can also see that the curve is not very consistent except at alignment and anti-alignment. The reason is the experiment points with 0.2 kV step showing an average effect, then the simulation is 0.01 kV step and 8000 points, which are more detailed.

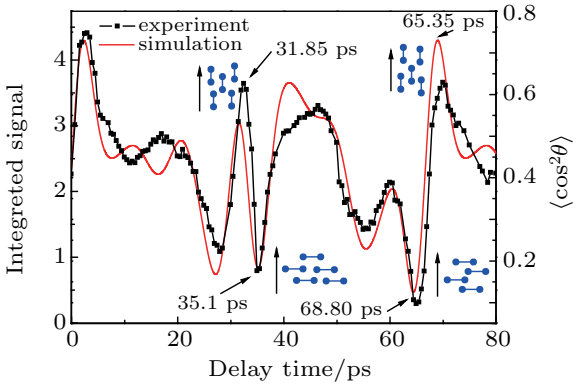


Fig. 3. Comparison in revival structure of CH_3I between simulated single rotation state of $|111\rangle$ (Fig. 1(b)) and measured normalized data, under the same condition. Arrow indicates laser polarization direction.

We have measured the 2D velocity distributions of I^+. Figures 4(a)–4(d) show the I^+ ions' images that are recorded at different pump-probe delay times in the revival for rotational-state-selected $|111\rangle$ molecules. We choose the delay times with maximum degree of the alignment and anti-alignment to be (a) $\tau=31.85$ ps, (b) $\tau=35.10$ ps, (c) $\tau=65.35$ ps, and (d) $\tau=68.80$ ps, respectively. The laser polarization vector is parallel to image plane. In Figs. 4(a) and 4(d) the distributions of I^+ ions are along the laser polarization vector, in Figs. 4(b) and 4(c) the distributions are perpendicular to the laser polarization vector. The alignment and anti-alignment are consistent with the scenarios in Fig. 3.

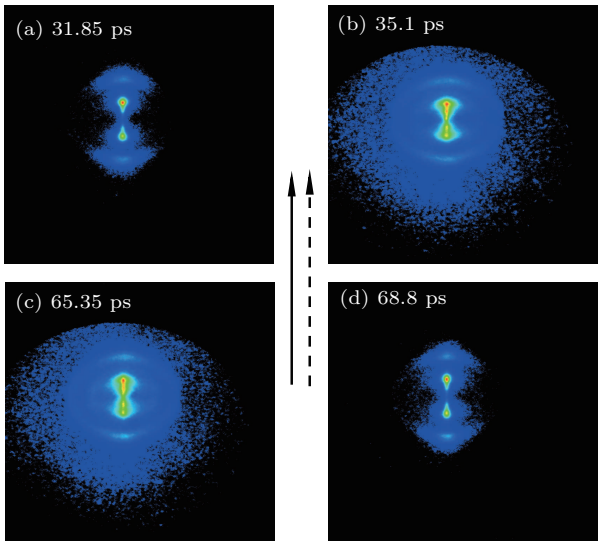


Fig. 4. Ion images of I^+ at different delay times: (a) $\tau=31.85$ ps, (b) $\tau=35.1$ ps, (c) $\tau=65.35$ ps and (d) $\tau=68.8$ ps. Arrow indicates laser polarization direction (pump and probe).

The inverse Abel transformation is crucial for the data analysis in photo-fragment-ion imaging and photo-electron imaging. For the Abel inversion, the BASEX algorithm has been employed.[36] This relates the Abel projected 2D radial and angular density distribution to the radial and angular density distribution in three-dimensional (3D) space, which reflects the alignment parameters. We obtain that the angular distribution is extracted from the outermost layer of the fragment-ion distributions due to the Coulomb explosion and the iodine fragments' angular distributions are shown in Fig. 5, which arise from the Coulomb explosion.

Figures 5(a) and 5(d) show the alignment angular distributions at half the revival delay time and full revival delay time, respectively. Most of molecules are parallel to the laser polarization direction, and the population peaks appear near the 0° and 180°. Figures 5(b) and 5(c) show the anti-alignment results. A number of molecules are populated perpendicularly to the laser polarization direction. Because the probe laser is parallel to the alignment pump laser, the molecular angular moments tend to be parallel to the probe laser. So the anti-alignment angular distributions' peaks are not fully populating near 90°. We compare the full revival angular distributions on the right graph, and alignment and anti-alignment are distinguishable.

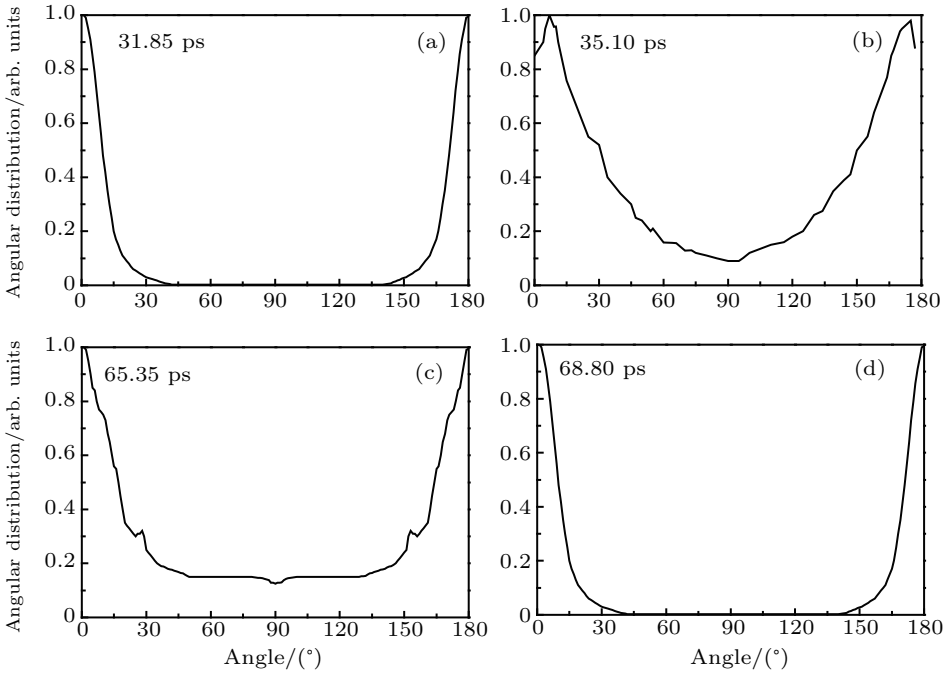


Fig. 5. Plots of I^+ angular distribution versus angle degree from alignment and anti-alignment.

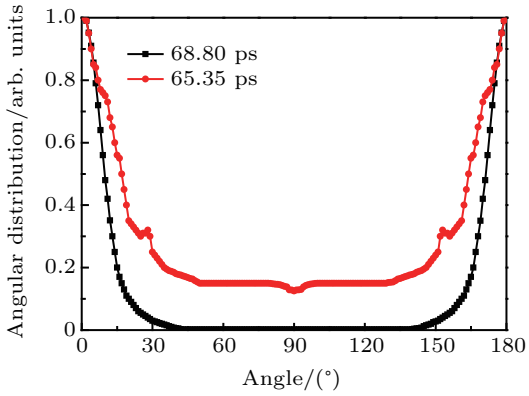


Fig. 6. Full revival angular distributions of I^+ at $t = 68.80$ ps for alignment (red) and at $t = 65.35$ ps for anti-alignment (black).

5. Conclusions

In this article, we have given a combined experimental and theoretical study on CH_3I alignment and we show the influence of the initial rotational-state populations. The CH_3I revival structures are compared between the single $|111\rangle$ rotation state simulation and the normalized experimental data. It is shown that high alignment degree can be obtained at cool temperature and pure rotational states.

Through experimental research, we obtain the CH_3I revival structures and find alignment and anti-alignment points. The experimental results are consistent with the simulation results. By the velocity map imaging technique, we obtain the I^+ ion velocity distributions and angular distributions, in which there appear the alignment and anti-alignment clearly at different pump-probe delay times. We can clearly observe the alignment and anti-alignment phenomena in the single image at a specific delay time. At the full revival time, the laser effect disappears completely and the molecules are under field-free conditions, so one can obtain the high degree alignment between 0.71 and 0.73. Theoretical simulation structure is consistent with the experimental results, and the alignment degree is estimated according to the experimental and simulation re-

sults.

This work provides the optimized molecular coordinate conditions for studying the cross molecular beams and collision experiments. From molecular coordinates' determination, we can better control the molecular space position. Our work provides critical conditions to study the higher harmonic, electronic information, molecular reaction dynamics, and molecular dynamics in depth. This paper is based on ion imaging. In the future we aim to observe images from electrons. At the same time, dynamic properties or processes can be further observed under the condition of alignment and anti-alignment. The spatial arrangement of molecules plays a crucial role. Facing the unique potential application of state selected and laser aligned molecular beams, it can be predicted that this kind of special molecular system has an important research value in the atom and molecule physics and chemistry. Future work is planned to find a kind of method that can be used to obtain the exact alignment degree directly.

Acknowledgment

The authors thank Liu Fu-Chun's group and Dr. He Lan-Hai for their helpful discussion.

References

[1] Mikosch J, Boguslavskiy A E, Wilkinson I, Spanner M, Patchkovskii S and Stolow A 2013 *Phys. Rev. L* **110** 023004
[2] Kanai T, Minemoto S and Sakai H 2007 *Phys. Rev. Lett.* **98** 053002
[3] Pinkham D and Jones R R 2005 *Phys. Rev. A* **72** 023418
[4] Li Y, Yang S P, Jia X Y and Chen J 2010 *Chin. Phys. B* **19** 043303
[5] Kramer K H and Bernstein R B 1965 *J. Chem. Phys.* **42** 767
[6] Bazalgette G, White R, Loison J C, Trénec G and Vigué J 1995 *Chem. Phys. Lett.* **244** 195
[7] Loison J C, Dur, A, Bazalgette G, White R, Audouard E and J 1995 *J. Chem. Phys.* **99** 13591
[8] Stapelfeldt H and Seideman T 2003 *Rev. Mod. Phys.* **75** 543
[9] Holmegaard L, Nielsen J H, Nevo I and Stapelfeldt H 2009 *Phys. Rev. Lett.* **102** 023001
[10] He L H, Bulthuis J, Luo S Z, Wang J, L U C J, Stolte S, Ding D J and Roeterdink 2015 *Phys. Chem. Chem. Phys.* **17** 24121
[11] Gandhi S R, Curtiss T J, Xu Q X, Choi S E and Bernstein R B 1986 *Chem. Phys. Lett.* **132** 6
[12] Kasai T, Fukawa T, Matsunami T, Che D and Ohashi K 1993 *Rev. Sci. Instrum.* **64** 1150
[13] Varma S, Chen Y H and Milchberg H M 2008 *Phys. Rev. Lett.* **101** 205001
[14] Ripoche J F, Grillon G, Prade B, Franco M, Nibbering E, Rüdiger E and André M 1997 *Opt. Commun.* **135** 310
[15] Wu J, Cai H, Peng Y, Tong Y, Couairon A, Tong Y Q and Zeng H P 2009 *Physics* **19** 1759
[16] Xu N, Li J and Zhang Z 2011 *ICEICE*, Vol. 03 (IEEE Computer Society Washington Distict of Columbia: InTech) pp. 606–609
[17] Averbukh I S and Perelman N F 1989 *Phys. Lett. A* **139** 449
[18] Robinett R W 2004 *Phys. Rep.* **392** 1
[19] Lee G H, Kim H T, Park J Y, Nam C H and Kim T K 2006 *J. Korkan Phys. Soc.* **49** 337
[20] Eppink A T J B and Parker D H 1998 *J. Chem. Phys.* **109** 4758
[21] Jung Y J, Yong S K, Kang W K and Jung K H 1997 *J. Chem. Phys.* **107** 7187
[22] van D B, Lipciuc M L and Janssen M H M 2003 *Chem. Phys. Lett.* **368** 324
[23] Samartzis P C, Bakker L G, Parker H and Theofanis N K 1999 *J. Phys. Chem. A* **103** 6106
[24] Graham P, Ledingham K W D, Singhai R P, Hankin S M and Mccanny T 2001 *J. Phys. B: At. Mol. Opt. Phys.* **34** 4015
[25] Seideman T 1995 *J. Chem. Phys.* **103** 7887
[26] Friedrich B and Herschbach D 1995 *Phys. Rev. Lett.* **74** 4623
[27] Yoshida M, Nakashima K and Ohtsuki Y 2015 *ICCMSE*, Vol. 1702 (Athens Greece: P Conference Proceedings) p. 1
[28] Hamilton E, Seideman T, Ejdrup T, Poulsen M D and Bisgaard C Z 2016 *Phys. Rev. A* **72** 440
[29] Zhu R H, Wang C C, Luo S Z, Yang X and Zhang M X 2013 *Front. Phys.* **8** 236
[30] Luo S Z, Zhou S S, HuW H, Li X K, MaP, Yu J Q, ZhuR H, Wang C C, Liu F C, Y B, Liu A H, YangY J, Guo F M and Ding D J 2017 *Phys. Rev. A* **96** 063415
[31] Luo S Z, Zhu R H, He L H, Wen HuW H, Li X K, Ma P, Wang C C, Liu F C, Roeterdink W G, Steven S and Ding D J 2015 *Phys. Rev. A* **91** 053408
[32] Anderson R W 1997 *J. Phys. Chem. A* **101** 7664
[33] Liu F C, Jin M X and Ding D J 2006 *Chin. Phys. Lett.* **23** 1165
[34] Roeterdink W G, Bulthuis J, Lee E P F, Ding D and Taatjes C A 2014 *Chem. Phys. Lett.* **598** 96
[35] Liu F C, Jin M X and Ding D J 2006 *Chin. Phys. Lett.* **23** 344
[36] Dribinski V, Ossadtchi A, Mandelshtam V A and Reisler H 2002 *Rev. Sci. Instrum.* **73** 2634